Dean&Francis
ISSN 2959-6157

Research on Swimming Stance Classification and Drowning Early Warning Technology Based on Acceleration Analysis

Zhewei Hu

Shenzhen College of International Education, Shenzhen 518048, China;

Abstract:

In this paper, we propose and validate a wearable device-based pool drowning early warning technology: a waterproof wristband based on Arduino intelligent development board is produced, and acceleration sensors and a wireless communication system are deployed on the wristband; the wristband sends the sensor data to the swimming pool early warning processing terminal; the terminal analyzes the acceleration data to complete the identification of the swimming posture, and makes an early warning of abnormal swimming posture and potential drowning behaviour, reminding the pool safety personnel to intervene. The above study shows that the drowning early warning program based on the waterproof bracelet and pool management terminal provides safety for swimmers and saves pool management costs, which has strong feasibility and great application potential.

Keywords: Swimming posture detection; Acceleration sensors; Wearable devices; Drowning warning.

1. Introduction

Drowning is a common unintentional injury, especially in the summer months or during seasons of high water activity. Swimmers need to closely watch their physical state during long hours of swimming or when physical exertion is high. Real-time monitoring of fatigue level, respiratory condition, and physical status can help detect symptoms of discomfort early and avoid drowning due to physical exhaustion, cramps, or other unexpected conditions. However, these essential precautions are often overlooked when swimming daily. Most of the drowning detectors on the market are based on visual detection and intelligent analysis. However, these technologies have limitations when facing crowds of people in the pool, underwater waves, light refraction, mirror fog, etc., making it difficult to analyze accurately. This paper proposes a drowning detection method based on a waterproof wristband acceleration sensor for drowning monitoring in a swimming pool environment. All swimmers wear waterproof wristbands that can transmit data in real-time, analyze the status of swimmers, and alarm in time when abnormalities are detected, calling safety personnel for confirmation and rescue. The method can effectively solve the current problems in drowning monitoring in swimming pools and optimize safety management.

Because of the small sample size and preexisting

ISSN 2959-6157

participant variances that create and magnify misleading mixed effects, current research on the structural and functional study of anxiety disorders typically yields contentious or inconsequential results. We used large samples of over 11,000 participants from the ABCD Study to minimize variability. We also used a linear mixed model (LMM) for data analysis to address the mixed impact caused by natural variance within the sample and increase the relevance and dependability of our findings.

This paper proposes a drowning detection method based on a waterproof wristband acceleration sensor for monitoring drowning in a swimming pool environment. All swimmers wear waterproof wristbands that can transmit data in real-time, analyze their status, and alarm when abnormalities are detected, calling safety personnel for confirmation and rescue. The method can effectively solve the current problems in drowning monitoring in swimming pools and optimize safety management.

2. Acceleration Sensor and Data Acquisition Technology Research

2.1 Acceleration Sensor

2.1.1 Acceleration sensor-based drowning warning system design

In this paper, a drowning warning system based on a waterproof wristband acceleration sensor is designed. The main idea is shown in Figure 1. Currently, swimmers wear waterproof wristbands distributed by swimming pools. This paper integrates three-axis acceleration sensors inside the waterproof wristbands to collect the acceleration signals of the wrists in the x, y, and z directions. The sensor acquires the motion data of the swimmer's wrist in real-time by sampling at a high frequency of 200 Hz and immediately transmits these signals to the data processor on the shore for preprocessing. The data processor first analyzes the three-axis acceleration signals in the time and frequency domains. Then, based on machine learning technology, it completes the classification of swimming posture recognition, warns about abnormal swimming posture, i.e., potential drowning behaviour, and calls the safety personnel to intervene.

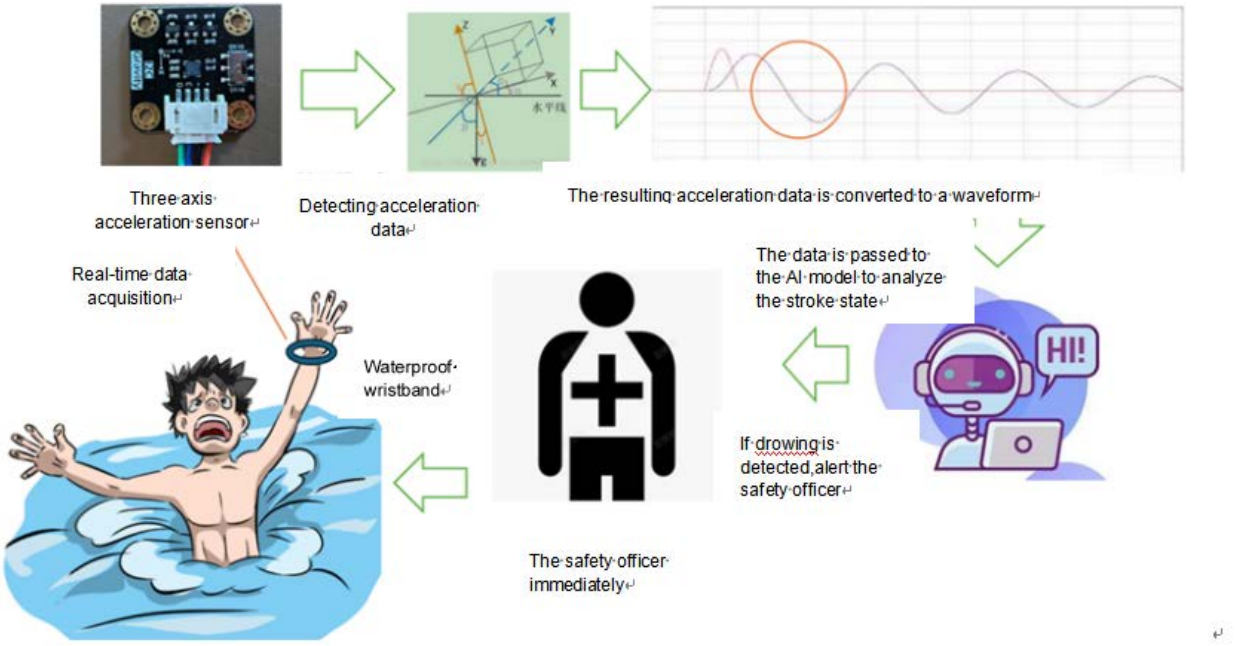

Fig. 1 Detection idea of drowning detection based on a waterproof wristband acceleration sensor.

2.1.2 Significant learnable correlation between acceleration signal characteristics acquired by triaxial acceleration sensors and drowning status

The hypothesis is validated if this study can capture and validate this correlation and effectively categorize the state using machine learning models. It has been shown

that the time-domain and frequency-domain features of acceleration signals can be used to recognize different movement states of the human body. Therefore, inputting these feature values into a machine-learning classification model can effectively distinguish between normal swimming posture, drowning posture, and other human behaviours in swimming pools. Only existing research has not yet focused on the analysis and detection of drowning behaviour; this study will focus on the goal of abnormal swimming posture detection to complete the data collection and data analysis and realize the drowning warning based on acceleration signal features.

2.2 Acceleration data acquisition

2.2.1 Data Acquisition Device

The Arduino control board serves as the core control unit of the system and is responsible for connecting and operating various microprocessors, controllers, and computers. According to the hardware design documents provided by the official Arduino website, we adjusted the board and components to meet the actual design requirements. On the Mind+ software platform, the acceleration data is captured through module programming, transferred to the computer for processing, and displayed on a connected display. The Arduino control board is easy to connect to sensors and various electronic components, supports various interactive programs, and is powered by a USB port, eliminating the need for an additional external power supply.

From Newton's second law, acceleration is determined by mass and force. Therefore, to measure the acceleration, connecting an object of constant mass to an elastic object, such as a spring that complies with Hooke's law at both ends and a displacement sensor on the other side, is sufficient. When a force is applied to the object, the spring expands and contracts, fed back to the displacement sensor, where the force on the spring is calculated from the object's displacement. Due to Newton's third law, the force on the object is known, which, when divided by its fixed mass, gives the acceleration at this point. MEMS technology can reduce this equivalent measurement principle to the device shown in Figure 2.

Therefore, acceleration can be measured in all three axes. In this project, the acceleration sensor used is the Gravity I2C LIS2DH three-axis acceleration sensor from DFRobot, as shown in Figure 3. The code allows the acceleration of the three axes to be output. A deflection was observed during the process of using the sensor, so it needed to be corrected by calculation. The Arduino code for 3-axis acceleration is as follows:

```
//Get the acceleration in the three directions of xyz
long ax, ay, az;
//The measurement range can be ±100g or ±200g set by the setRange() function
ax = acce.readAccX(); //Get the acceleration in the x direction
ay = acce.readAccY(); //Get the acceleration in the y direction
az = acce.readAccZ(); //Get the acceleration in the z-direction
//Print acceleration
Serial.print(\"Acceleration x: \");
Serial.print(ax);
Serial.print(\" mg/t y: \");
Serial.print(ay);
Serial.print(\" mg/t z: \");
Serial.print ln(az);
delay(300);
```

The measured x-axis, y-axis, and z-axis acceleration values need to be converted to a real-life human body coordinate system, where the x1 axis is forward along the coronal side of the body, the y1 axis is to the left, and the z1 axis is downward on the horizontal side. At this point, the direction of the z1 axis is consistent with the direction of the gravitational acceleration g. The direction of the new coordinate system will not change with the person's movement. The measured values of the three axes are mapped to the new coordinate axes, and the sum of the squares of x1, y1, and z1 measured by the sensor at rest should be equal to the square of the acceleration of gravity g.

ISSN 2959-6157

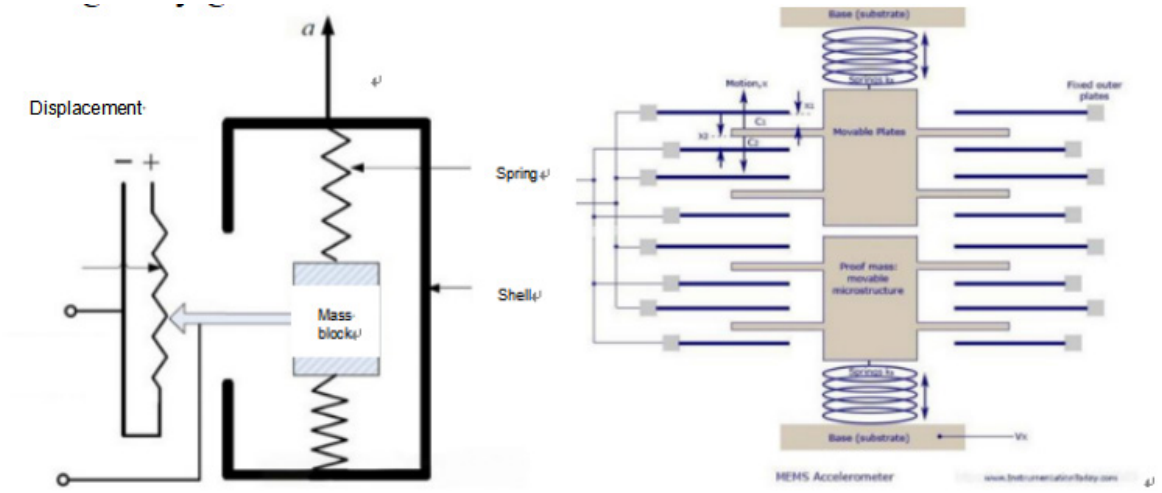

Fig. 2 Schematic of uniaxial acceleration (left) Acceleration measurements in MEMS technology (right)

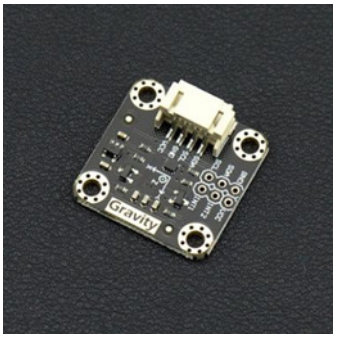

Fig. 3 Physical drawing of the triaxial sensor.

2.2.2 Data Acquisition Procedure

Therefore, the acceleration data collection for this experiment includes data collected from the own device and the public database. The device data comes from the data collected in a hotel swimming pool in Shenzhen during the summer of 2024, and the public database uses the IMU dataset of swimming strokes provided on the Kaggle platform. The public dataset contains data from IMUB sensors, recording the readings of accelerometers, gyroscopes, and magnetometers while swimming, and we only select the reading changes of their accelerometers. The experimental data acquisition process and results are shown in Figure 4. The data recording time for each swimming stroke is a few seconds. The detailed dynamic characteristics of various swimming postures can be obtained as control data under normal conditions.

After the data collection, the drowning and standard swimming stroke data will be merged, disordered, and labeled as different swimming strokes. Subsequently, the data will be divided into a training set and a validation set, in which 70% will be used to train the machine learning model, and 30% will be used to validate the model's performance. Through this approach, the accuracy and reliability of the drowning detection system can be effectively improved, and the algorithm's performance in different states can be thoroughly evaluated. The final analysis results will provide the necessary data to support the optimization of the drowning detection algorithm.

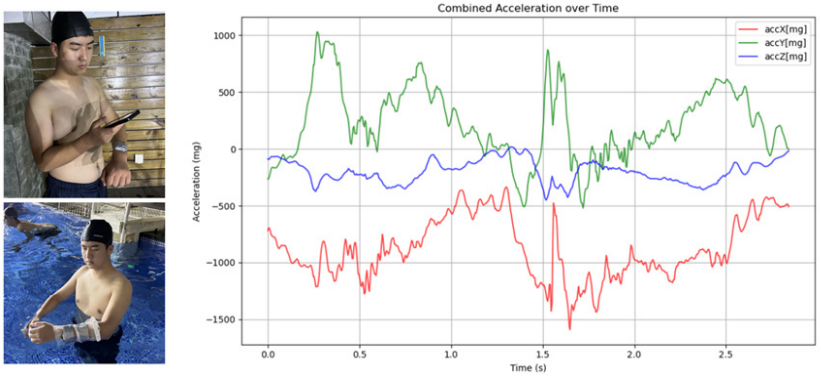

Fig. 4 Acquisition process and results of triaxial acceleration data

2.3 Preprocessing and feature extraction of acceleration signals

2.3.1 Acceleration Signal Preprocessing

The quality of acceleration signals in everyday life is lower than that of precise wristband acceleration data used in lab settings because they are more vulnerable to interference from shifting water currents, inappropriate wear, and other variables. Preprocessing these acceleration signals, therefore, aids in obtaining a higher-quality waveform view. This experiment employed four primary preprocessing techniques: baseline deduction, filtering, and gravity removal. These methods aim to improve the precision and stability of the signals, enhancing the data analysis's reliability. After the base data preprocessing, the acceleration signal data already had fundamental integrity and dependability. We have successfully increased the data's readability and clarity by eliminating the gravity component, using Kalman filtering, and processing baseline deductions. By optimizing the signal quality and providing a strong basis for the feature extraction process, these preprocessing processes make it possible to perform more precise and efficient data analysis and model building.

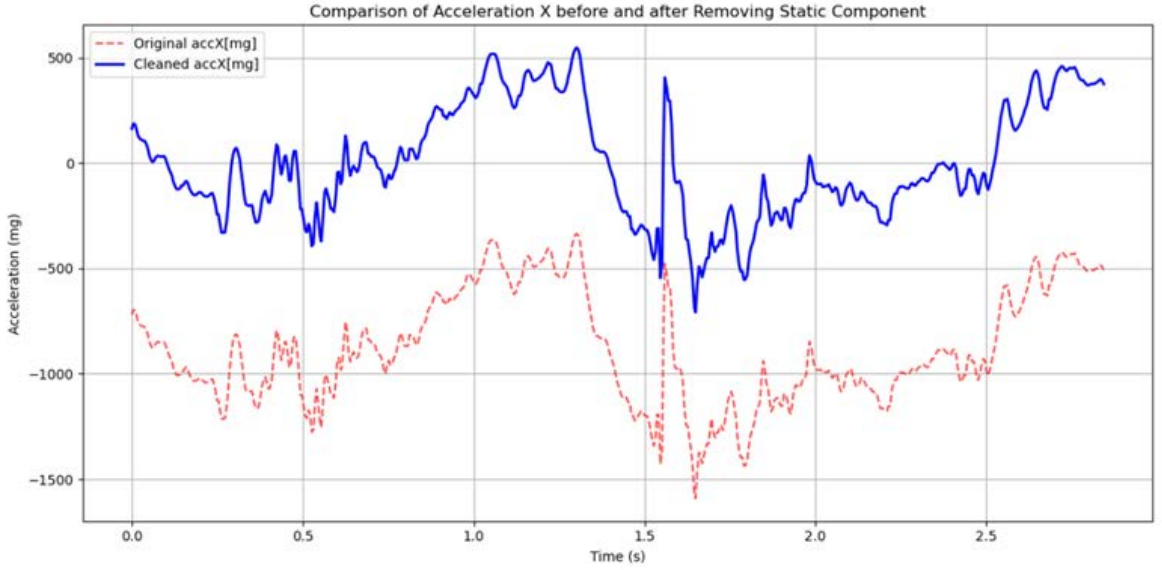

Fig. 5 Comparison before and after gravity removal (the blue solid line is after gravity removal, and the red dashed line is original data)

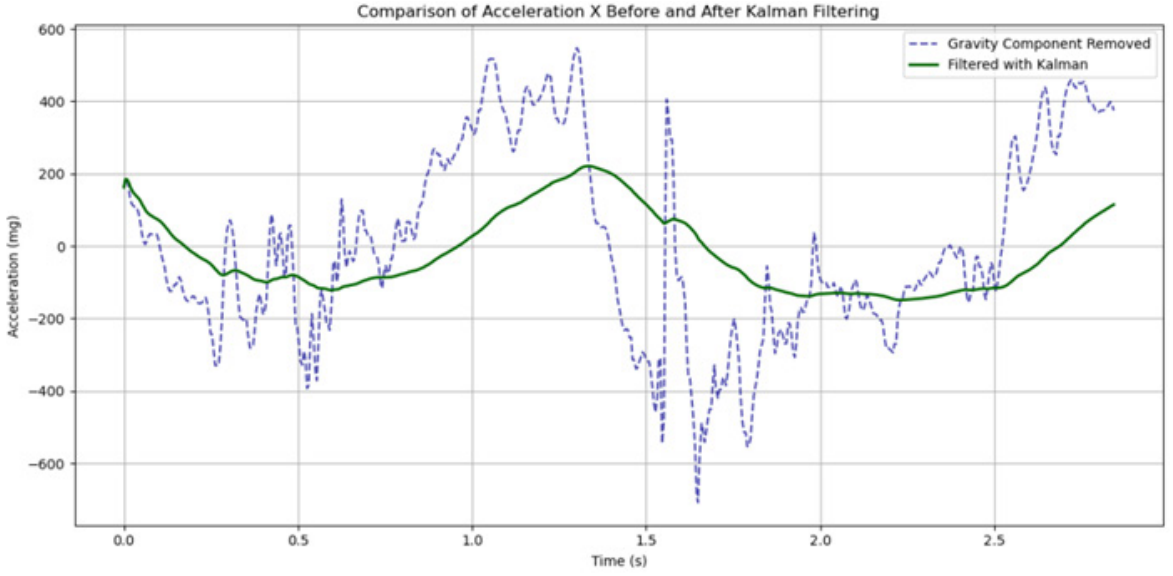

Fig. 6 Comparison of waveforms before and after Kalman filtering (green solid line is after filtering, blue dashed line is before filtering)

ISSN 2959-6157

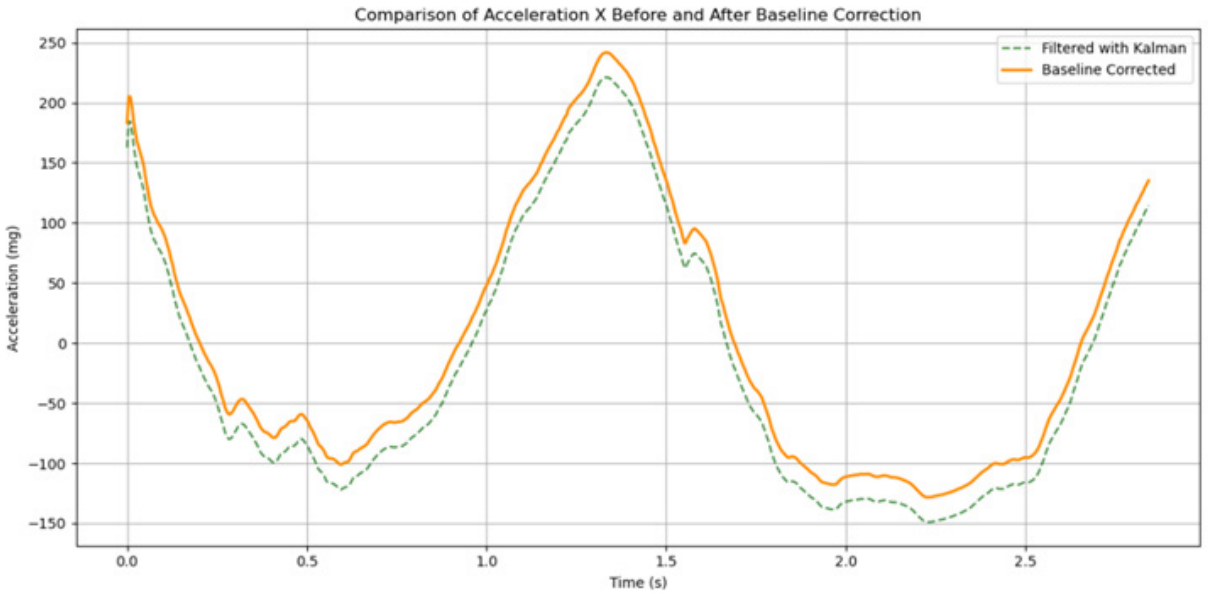

Fig. 7 Comparison of waveforms before and after baseline deduction (green dashed line is before deduction, yellow solid line is after deduction)

2.3.2 Extraction of the main motion axes

First, we subjected the acceleration signals to a preprocessing step, including removal of the gravity component, Kalman filtering, and baseline deduction, followed by the x-, y-, and z-axis accelerations within each time window. These acceleration values are then plotted into a graph chronologically to show the changes in x, y, and z-axis acceleration within a single time window. By combining these data into a single plot for comparison, as shown in Figure 8, it was observed that there was no significant difference between the acceleration signals in different axial directions.

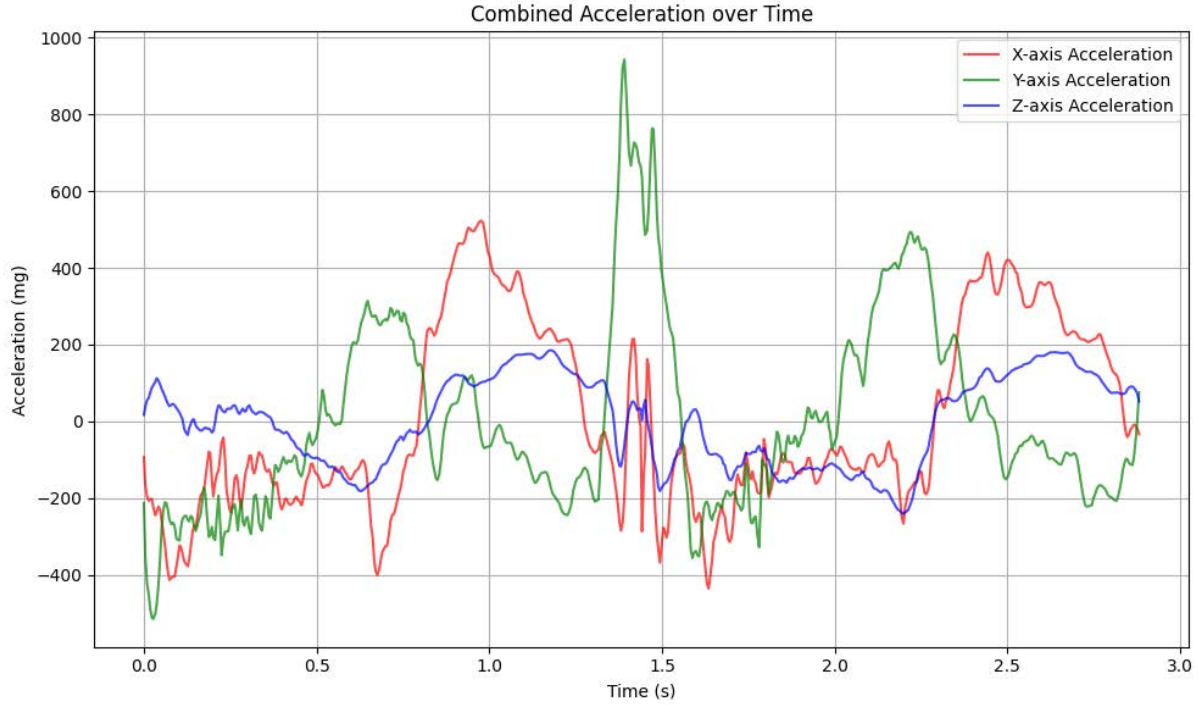

Fig. 8 Demonstration of three-axis acceleration in a time window after preprocessing

As seen in Figure 8, an accurate judgment cannot be drawn by only observing the triaxial acceleration of one

swim stroke in a single time window. We randomly selected 10-time windows from a single stroke to more comprehensively analyze the acceleration characteristics of different swim strokes. For the uniaxial acceleration data within these time windows, we plotted them in the same graph to compare the consistency of the acceleration data within different time windows, as shown in Fig. 9:

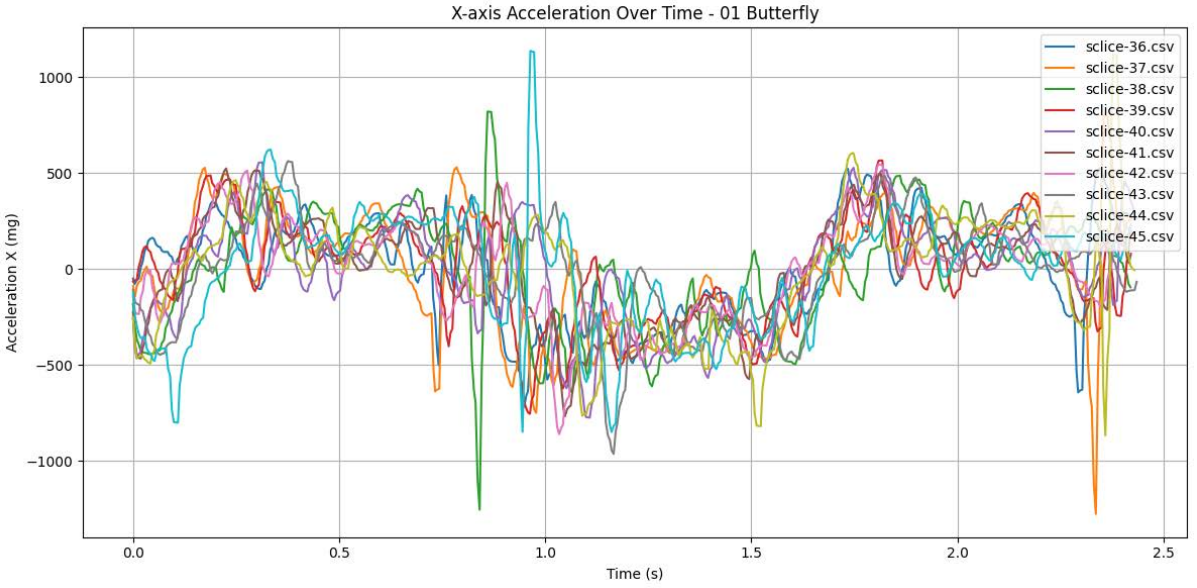

Fig. 9 Consistency comparison of uniaxial acceleration data in ten randomly selected time windows

By looking at the images, it can be seen that the acceleration data for the same axis exhibits consistency for the most part over a single period. However, at certain moments, the data performance appeared more chaotic. Further analysis shows that this confusion mainly stems from the differences in the movement's onset time and the stroke's completion phase within different time windows. These differences in time windows led to variability in the acceleration data, which affected the coherence of the overall image.

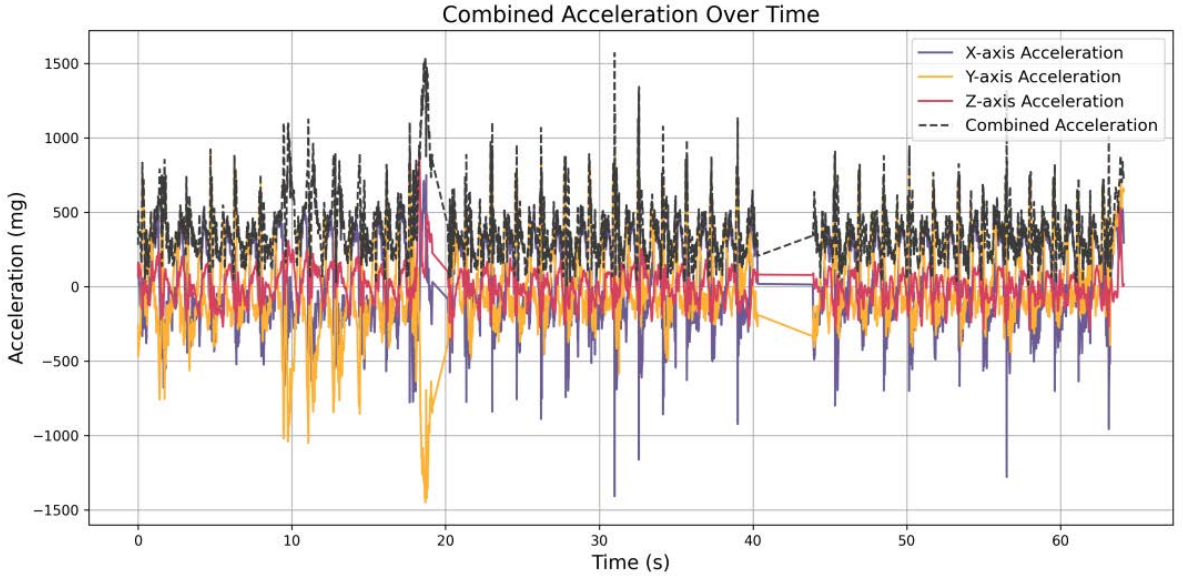

Fig. 10 Composite of triaxial acceleration and combined acceleration data during a complete single swim stroke

In analyzing the three-axis acceleration and the combined acceleration data during a single motion cycle, Figure

ISSN 2959-6157

11 shows the relationship between the x- and y-axis and combined acceleration. The figure shows that the x-axis and y-axis accelerations are closer to the combined acceleration in the overall trend. At the same time, the z-axis has relatively less influence. However, in the actual image, the specific contribution of the x-axis and y-axis acceleration to the combined acceleration is still not easy to distinguish. Although the x-axis and y-axis acceleration data show some correlation with the combined acceleration, it is difficult to identify which axial acceleration has a more significant effect on the combined acceleration in the graphs. Further analysis and processing are required to more clearly identify the specific contribution of each axial acceleration to the overall state of motion.

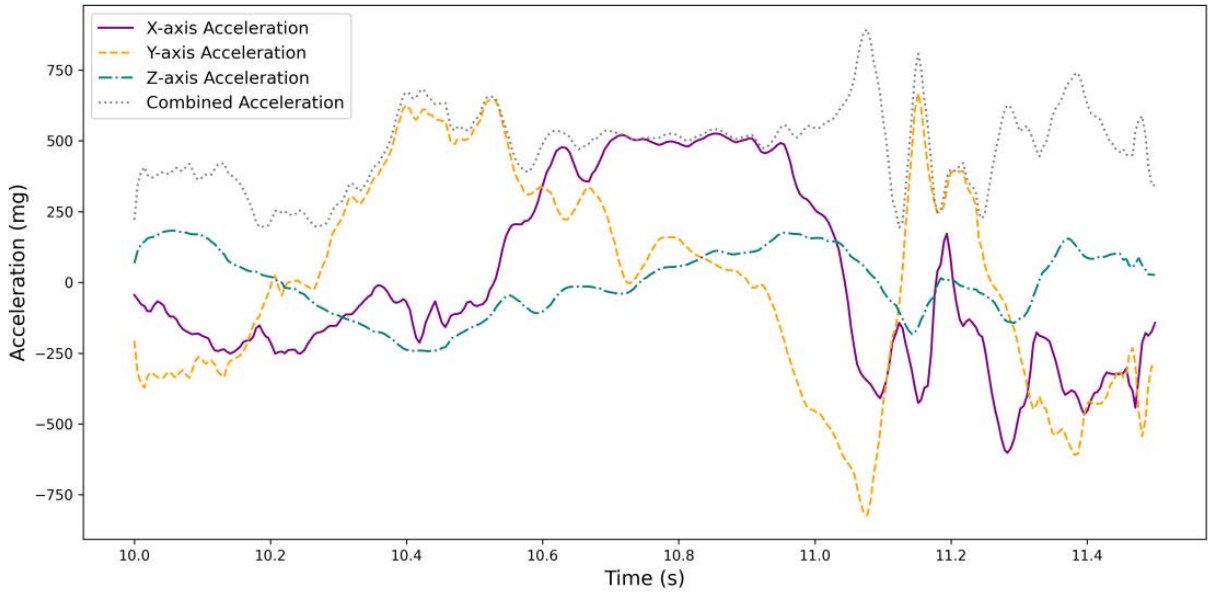

Fig. 11 Plot of triaxial acceleration versus combined acceleration for a single cycle of motion

To further investigate the weighting of the triaxial acceleration on the combined acceleration, we will mathematically quantify the difference between the acceleration of each axis and the combined acceleration to compare the weighting with the combined acceleration. It will be done by using the entire course of a single stroke and calculating the effect of each axis (x-, y-, and z-axis) on the combined acceleration. We define this difference as follows:

$$\text{Difference}_x = \frac{1}{N}\sum_{i=1}^{N}\left(\sqrt{x_i^2 + y_i^2 + z_i^2} - |x_i|\right) \quad (1)$$

$$\text{Difference}_y = \frac{1}{N}\sum_{i=1}^{N}\left(\sqrt{x_i^2 + y_i^2 + z_i^2} - |y_i|\right) \quad (2)$$

$$\text{Difference}_z = \frac{1}{N}\sum_{i=1}^{N}\left(\sqrt{x_i^2 + y_i^2 + z_i^2} - |z_i|\right) \quad (3)$$

Where N is the sample size, "x_i," "y_i," and "z_i" are the acceleration data at the time point. The higher the difference, the lower the fit between the acceleration data of this axis and the combined acceleration, meaning that the overall influence of this axis on the combined acceleration is more negligible. Conversely, the lower the difference, the more significant the effect of the acceleration data of this axis on the combined acceleration, which is the main factor in judging the swimming posture. Thus, by analyzing these differences, we can more accurately identify the axes with the most significant influence on the motion state.

By plotting the mean values of the calculated differences in triaxial acceleration in different swim strokes into a single graph, as shown in Figure 12, it is possible to observe the differences in the influence of each axis in different swim strokes. This graph demonstrates the relative contribution of each axis to the combined acceleration and reveals the extent to which each axis contributes to the combined acceleration in different swim strokes. Despite the differences between the axes demonstrated in the figure, it may still be challenging to identify which axis has the most significant effect. Therefore, further analysis is required to determine the axes with the most significant impact on the combined acceleration and assess their importance in the overall kinematic state.

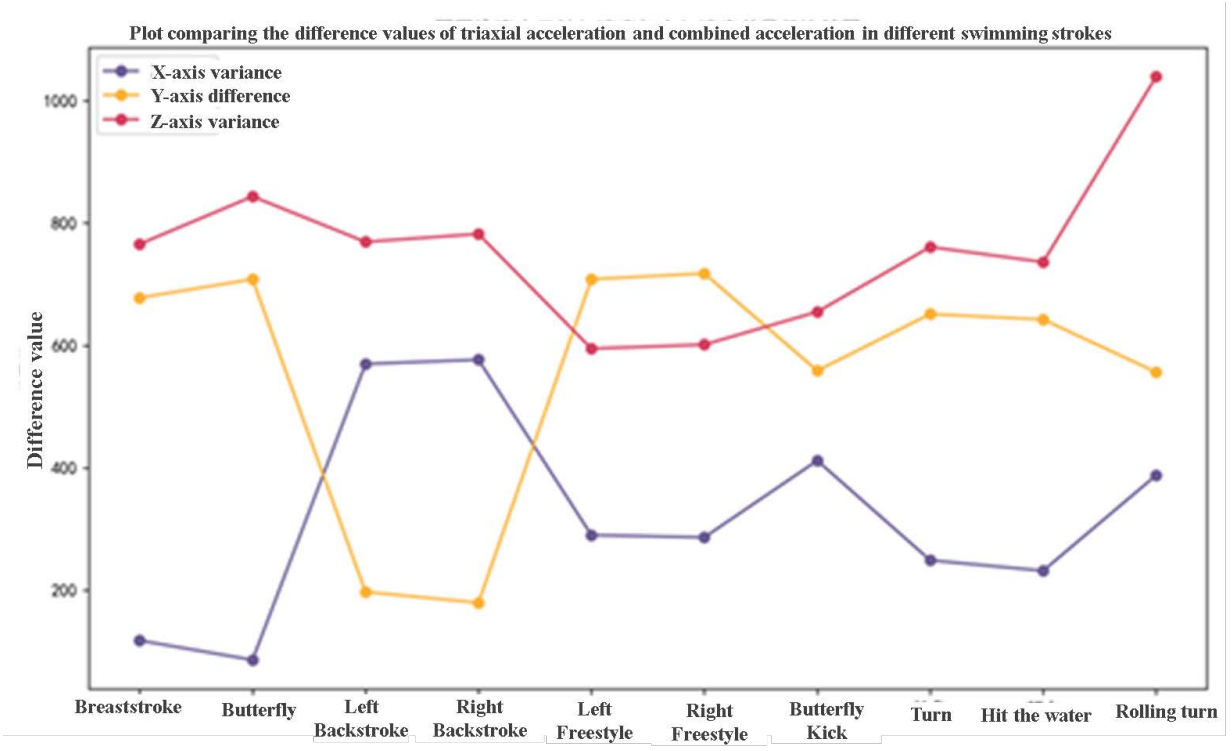

Fig. 12 Comparison of the difference values of triaxial acceleration and combined acceleration in different swimming strokes

To fully assess the overall effect of triaxial acceleration on combined acceleration, we calculated the mean value of the difference between triaxial acceleration and combined acceleration for all the different swim strokes. This approach allowed us to identify which axial direction had the most significant effect on the combined acceleration across all stroke conditions. By aggregating these means, we can locate the axial direction with the most significant impact on the combined acceleration and further analyze its relative importance in the overall motion state. The table below shows the difference between the mean values of the acceleration of each axis and the combined acceleration for all swimming positions, and the results show that the difference between the y-axis acceleration and the combined acceleration is relatively tiny.

Table 1 Mean differences between triaxial acceleration and combined acceleration for all swim strokes

axis	mean difference
x	276.13
y	249.24
z	341.73

Based on this finding, we hypothesize that y-axis acceleration is essential in determining drowning. Higher weights can be assigned to the y-axis acceleration during machine learning to verify this viewpoint and observe whether it significantly improves the drowning detection performance after assigning higher weights to the y-axis acceleration to optimize the detection effect of the model. In practical applications, the XYZ relationship may change. However, the above method can still extract the central motion axis with the most significant influence and does not affect the subsequent discussion.

2.3.3 Acceleration signal time domain feature extraction

After determining the primary axis of motion, the time domain feature extraction of the signal can begin. Ordinary time domain features include mean, variance, standard deviation, correlation coefficient, first quartile, maximum and minimum values. In addition, features describing the details of the signal waveform, such as the root mean square, autoregressive coefficient, skewness, kurtosis, and over-zero rate, can also be computed. In this paper, the

ISSN 2959-6157

following time-domain features will be used for analysis: mean, variance, skewness, kurtosis, correlation coefficient, and first quartile.

2.3.4 Acceleration signal frequency domain feature extraction

Since acceleration signals can reveal their frequency components and energy distribution in the frequency domain, performing frequency-domain feature extraction can help better understand the signal's periodic and spectral properties. Frequency-domain feature extraction requires converting a Fourier transform of the signal to a frequency-domain representation. The following are the spectrograms generated for different swimming strokes after the Fourier transform.

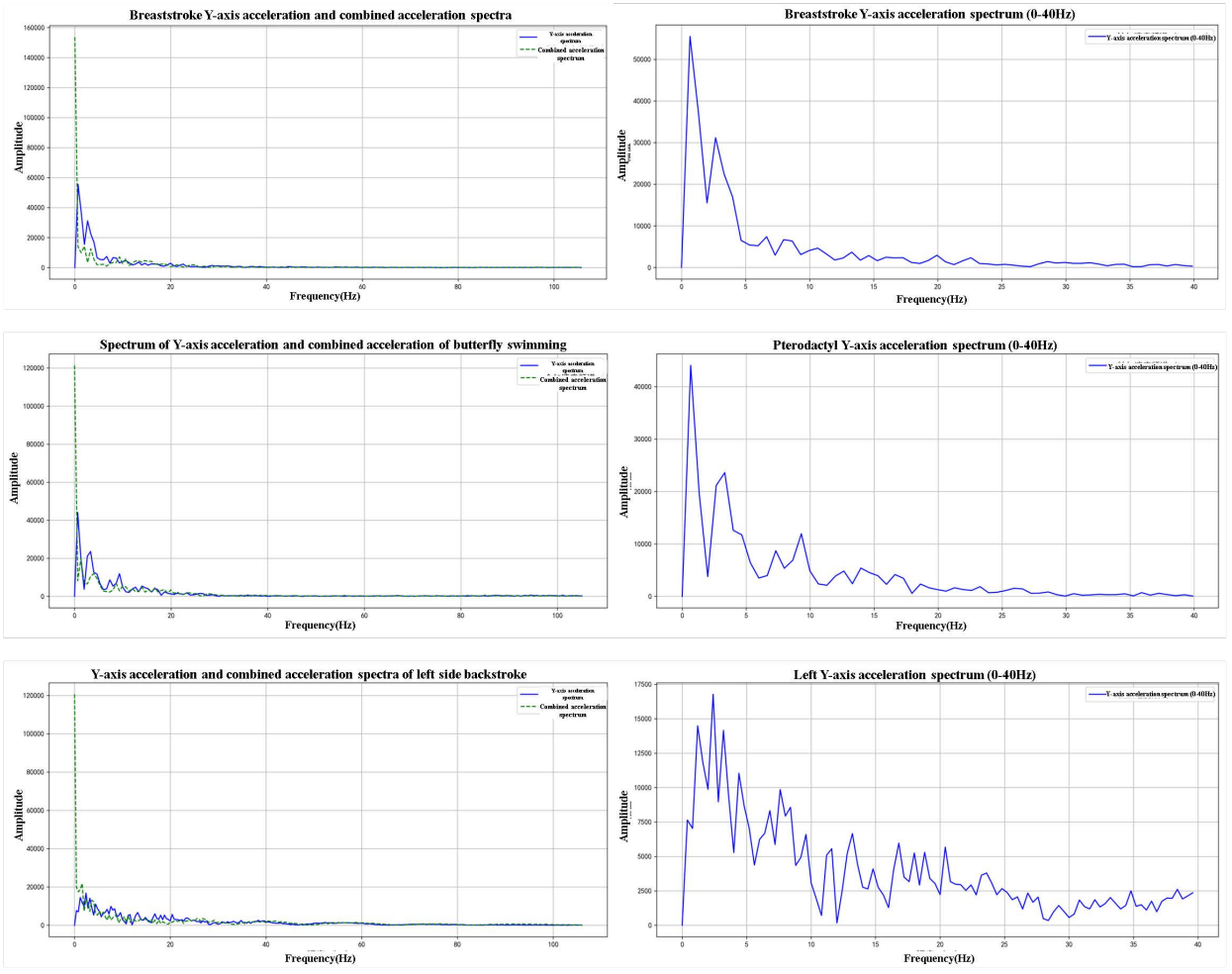

Fig. 13 Spectrograms of Y-axis acceleration vs. combined acceleration for breaststroke, butterfly, and left-side backstroke.

Unlike time-domain feature extraction, frequency-domain feature extraction can provide information about the signal's frequency distribution, frequency concentration, and spectral shape. This paper will use frequency-domain features such as primary frequency, the spectral center of mass, spectral bandwidth, spectral flatness, spectral roll-off point, spectral entropy, and spectral energy.

3. Research on intelligent recognition technology of swimming posture

3.1 Machine Learning Models for Swimming Stance Classification

To fully explore the potential information in the data and achieve efficient classification tasks, this project analyzes four commonly used machine learning models: Support Vector Machine (SVM), K-Nearest Neighbor Algorithm (KNN), Decision Tree, and Random Forest. These models

are selected based on their effectiveness and wide application in classification problems.

SVM (Support Vector Machine) is a robust supervised learning algorithm mainly used for classification and regression tasks. The basic idea is to classify data into different classes by finding an optimal hyperplane.SVM separates samples of other classes as much as possible by finding a hyperplane that maximizes the boundary distance (i.e., spacing) in a high-dimensional feature space. To improve the classification accuracy, SVM uses kernel functions (e.g., linear kernel, polynomial kernel, RBF kernel, etc.) to map the original data to a higher dimensional space so that an appropriate decision boundary can be found even under more complex data distributions.SVM has a good generalization ability, which is especially suitable for the classification problem of small-sample datasets, and its performance is excellent in high-dimensional space.

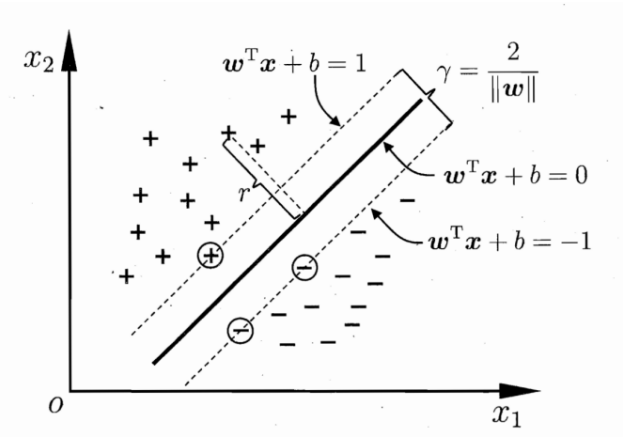

Fig 14 Support vectors and intervals.

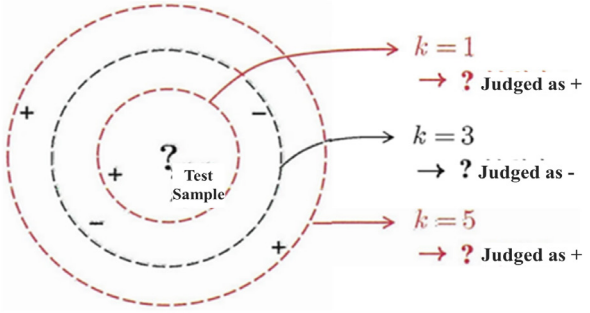

Fig. 15 K-nearest neighbor classifier.

KNN (K-Nearest Neighbors, K-Nearest Neighbors Algorithm) is an instance-based learning method whose core idea is to classify samples by comparing their distances. Given a sample to be classified, KNN first calculates the distance between this sample and all the samples in the training set (usually using the Euclidean distance) and then selects the K samples closest to it as the reference point. Finally, based on the category information of these K samples, the category of the sample to be classified is determined by the principle of majority rule. The KNN algorithm is simple and easy to use, does not need to train the model explicitly, and has a high degree of interpretability. However, KNN is less suitable for high-dimensional data and has higher computational complexity, especially when the data volume is significant, so classification performance may be significantly affected.

A decision tree is a tree-structured classification model whose basic idea is gradually splitting the data set into smaller subsets through a series of judgment rules. In constructing decision tree models, metrics such as information gain, gain rate, or Gini coefficient are usually used to select the optimal segmentation features to minimize the data's uncertainty. The decision tree model is intuitive, easy to understand, and suitable for dealing with data with nonlinear relationships. However, it is prone to overfitting. To improve the generalization ability, it is usually necessary to prune the decision tree or use it in combination with other integration methods.

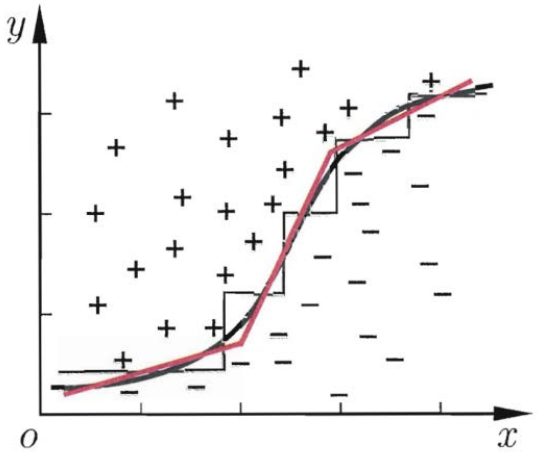

Fig. 16 Schematic representation of the approximate classification boundary of the decision tree.

3.2 Optimization of swim stroke classification algorithm based on acceleration features

This paper uses the above four models to train the sample data respectively. The training data and test data are divided into a ratio of 7:3, with 70% of the training data and 30% of the test data. The data labels are divided into normal swimming posture and drowning situation. According to the difference in extracted features, three datasets are constructed in this paper: the one containing only time-domain features, the one containing only frequency-domain features, and the one containing both time-domain and

ISSN 2959-6157

frequency-domain features. The test results of each model on different datasets after training are shown in Table 1. This paper uses Precision, Recall, and F1 Score as the primary evaluation metrics.

Precision, recall, and F1 scores are based on a weighted average of the two labels (everyday swimmer and drowning condition) to prevent the evaluation of the model from being affected by data imbalance. Precision indicates the proportion of samples predicted by the model to be in the positive category that are actually in the positive category, and recall suggests the proportion of samples that are actually in the positive category that are correctly predicted to be in the positive category. The F1 score is the reconciled mean of precision and recall, which strikes a balance between precision and recall and is particularly suitable for datasets that are not balanced in category.

Table 2 Classification performance evaluation of four models on different feature datasets

Type of data set	mould	Unenhanced y-axis features			Enhanced y-axis features		
		precision	recall rate	F1 score	precision	recall rate	F1 score
Time-domain features only	SVM	0.88	0.87	0.87	0.88	0.87	0.87
	KNN	0.80	0.79	0.78	0.84	0.81	0.81
	decision tree	0.86	0.81	0.83	0.86	0.84	0.84
	random forest	0.88	0.86	0.86	0.91	0.91	0.90
Frequency domain features only	SVM	0.85	0.84	0.84	0.88	0.87	0.87
	KNN	0.73	0.71	0.71	0.76	0.72	0.72
	decision tree	0.90	0.85	0.86	0.89	0.88	0.88
	random forest	0.92	0.92	0.92	0.94	0.93	0.93
Time & Frequency Domain Characterization	SVM	0.90	0.90	0.89	0.91	0.90	0.90
	KNN	0.84	0.83	0.83	0.83	0.83	0.83
	decision tree	0.88	0.87	0.87	0.88	0.87	0.87
	random forest	0.95	0.94	0.94	0.97	0.95	0.96

The results show that the Random Forest model performs well on all f precision, recall, and F1 score datasets. That is because Random Forest can effectively deal with high dimensional and large-scale data, successfully capturing complex patterns in the data by randomly selecting features and integrating multiple decision trees. On the contrary, KNN performs relatively poorly on all datasets. That is because KNN relies on the distance between samples for classification. When the dataset has high dimensionality or the samples are unevenly distributed, KNN is susceptible to "dimensionality catastrophe," which reduces the classification performance.

Meanwhile, after enhancing the y-axis features, we observe that the model significantly improves precision, recall, and F1 score in 85% of the cases, as shown in Fig. 17. This result indicates that y-axis acceleration plays a vital role in discriminating drowning situations. By strengthening the weights of the y-axis features, we can recognize drowning events more effectively, thus improving the model's overall performance. This further validates the effectiveness of y-axis acceleration as a key feature in drowning detection.

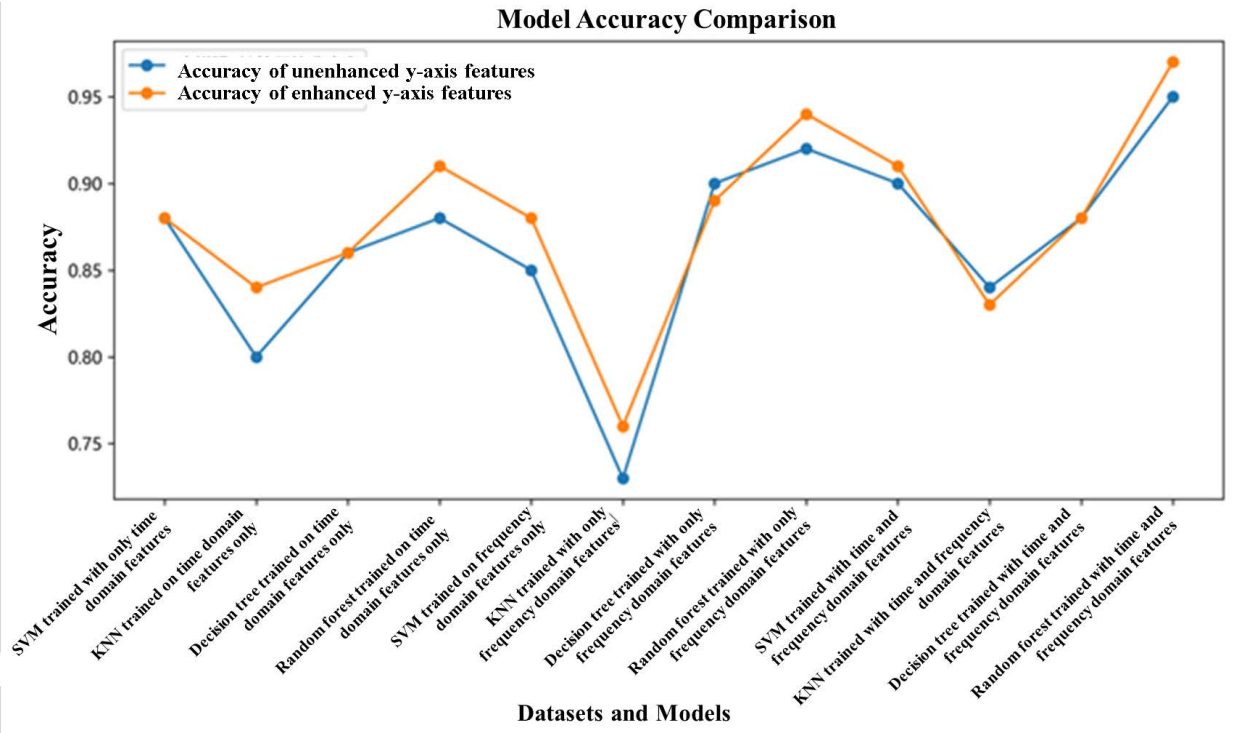

Fig. 17 Comparison of accuracy of different models before and after y-axis feature enhancement.

The aforementioned experimental results show that the feasibility of the research methodology and hypotheses proposed in this paper in the task of drowning detection has been preliminarily validated. Although the performance of different models varies on specific datasets and feature combinations, in general, a variety of commonly used machine learning models show potential for application in drowning detection in terms of accuracy, recall, and F1 score. Particularly noteworthy is that the random forest model achieves 97% accuracy on a dataset containing both time and frequency domain features. That study has an enormous scope for development and potential applications.

4. Conclusion

Fast and timely handling of drowning is crucial for timely implementation of rescue measures, and the early warning scheme based on three-axis acceleration sensor data analysis in this paper has strong application potential. In this study, we preprocessed the swimming acceleration data based on self-collected data and public databases. We extracted time-domain and frequency-domain angular features from the main motion axes. We compared and optimized the results of swimming stroke recognition from various machine learning models. This paper proposes an innovative early warning processing scheme for drowning, which utilizes acceleration sensors in waterproof wristbands worn by ordinary users to achieve real-time monitoring. This approach provides a new technical means for the traditional drowning prevention technology, enabling drowning detection to be more conveniently integrated into daily life. This study analyzes and enhances the usefulness of acceleration data features in intelligent recognition techniques for swimming strokes, based on which the accuracy of stroke recognition can be improved to 97%, which helps to differentiate between regular swimming strokes and drowning situations. This paper provides insights into the field of drowning detection techniques by exploring the performance of different machine learning models on time and frequency domain feature sets.

References

[1] Van Beeck EF, Branche C M, Szpilman D, et al. A new definition of drowning: towards documentation and prevention of a global public health problem[J]. Bulletin of the World Health Organization, 2005, 83: 853-856.

[2] Grmec Š, Strnad M, Podgoršek D. Comparison of the characteristics and outcome among patients suffering from out-of-hospital primary cardiac arrest and drowning victims in cardiac arrest[J]. International journal of emergency medicine, 2009, 2: 7-12.

[3] G.X. Zhao, W.K. Chen. A review of drowning alarm systems research in swimming pools [J]. Instrumentation User, 2005,

ISSN 2959-6157

12(3):2. DOI:10.3969/j.issn.1671-1041.2005.03.001.

[4] Xiu-Nian Zhang. Research on drowning warning in swimming pools based on attitude estimation and edge computing [D]. Shanghai: Donghua University,2022.

[5] Xue Y, Jin L. A naturalistic 3D acceleration-based activity dataset & benchmark evaluations[C]//2010 IEEE International Conference on Systems, Man and Cybernetics. I.e., 2010: 4081-4085.

[6] Wu Hailong. Analysis and realization of a swimming monitoring system based on acceleration sensor [D]. South China University of Technology [2024-08-30].DOI:CNKI:CDMD:2.1018.875115.

[7] Mooney R, Corley G, Godfrey A, et al. Inertial sensor technology for elite swimming performance analysis: a systematic review[J]. Sensors, 2015, 16(1): 18.